Investigating the Impact of Ambient Temperature on MOSFET in BUCK Converters, SEPIC Converters, and Power Supply PCB Board (June 2023)

Suhaib Abugdera[1], St. Cloud State University, Prof. Mahbub Hossain[2], St. Cloud State University

***Abstract*— This paper undertakes a comprehensive exploration of the impact of ambient temperature on MOSFET transistor performance and reliability within the contexts of BUCK converters, SEPIC converters, and power supply printed circuit board (PCB) applications. Combining theoretical analysis, computer simulations, and experimental testing, this research scrutinizes how ambient temperature variations influence the electrical parameters of MOSFETS and the output voltage of the circuit, including key facets like voltage and current ratings, and thermal stability. The study further probes the effects of these temperature changes on the efficiency and power density of different converter topologies, such as BUCK and SEPIC converters. Experimental findings highlight significant alterations in transistor performance characteristics due to temperature shifts, leading to consequential changes in the efficiency, stability, and reliability of associated converters and power supply PCBs. To counter these temperature-induced effects, the paper proposes a range of design strategies and thermal management techniques aimed at enhancing the performance and longevity of power electronic systems. Ultimately, this research provides valuable insights into the role of temperature in the performance and reliability of the circuits contains MOSFETS in power electronics, aiding the ongoing evolution of robust, efficient, and reliable converters and power supply PCBs across various industries.**

***Index Terms*—Analog Digital Converter (ADC), Altium Designer, Ambient Temperature (Ta), Buck Converter, Celsius (˚C), Continuous Current Mode (CCM), Heat Sink, Input Voltage (V_{in}), LM35 Temperature Sensor, LTC3850 Controller, LTSpice, Metal-Oxide Semiconductor Field-Effect Transistor (MOSFET), Output Voltage (Vout), Printed Circuit Board (PCB), Polygon Pour, Single-Ended Primary Inductor Converter (SEPIC), Temperature Coefficient of Capacitance (TCC), Temperature Coefficient of Resistance (TCR), Thermal Vias.**

This work was supported by St. Cloud State University, and in part by the ECE research class at St. Cloud State University. (Corresponding authors: Suhaib F. Abugdera. Md Mahbub Hossain.)

[1] Suhaib Abugdera was a student in St. Cloud State University, St. Cloud, MN 56301 USA. (e-mail: Suhaib.Abugdera@go.stclodstate.edu).

[2] Mahbub Hossain is a professor and chair of Electrical and Computer Engineering Department, St. Cloud State University, St. Cloud, MN 56301 USA. (e-mail: mmhossain@stcloudstate.edu).

I. Introduction

Temperature plays a crucial role in determining the performance and reliability of power electronic systems, particularly in applications involving transistors, such as BUCK converters, SEPIC converters, and power supply printed circuit board (PCB) designs. Understanding and managing the impact of temperature on these systems is essential for optimizing their efficiency, stability, and longevity. This research aims to investigate the effects of temperature on MOSFET transistors in various converter topologies and power supply PCBs, providing valuable insights and recommendations for design improvements and thermal management techniques.

To achieve this objective, a series of experiments and simulations were conducted using both through-hole and surface mount components on PCBs. Hot air was employed to heat the circuits in a controlled manner and ice bag was also used to cool down the temperature to about 0˚C, simulating the thermal conditions experienced by the MOSFET during operation. Temperature measurements were taken using LM35 temperature sensors, with an Arduino Uno employed to convert the analog voltage output to temperature values in Celsius. Voltage measurements were performed using a multimeter, allowing for the accurate evaluation of circuit parameters under varying temperature conditions.

The BUCK and SEPIC converters were designed and simulated using calculations from relevant textbooks, ensuring that the selected topologies were consistent with established theory and best practices. LTSpice was used to perform the simulations, providing a reliable platform for assessing the converters' performance and behavior under different thermal conditions. For the power supply PCB design, a typical example from the LTC3850 datasheet was utilized, ensuring compliance with industry standards and guidelines. The PCB was designed using Altium Designer, a widely recognized and powerful tool for PCB layout and design.

By combining experimental testing, theoretical analysis, and computer simulations, this research offers a comprehensive assessment of the impact of ambient temperature on MOSFETs in BUCK converters, SEPIC converters, and power supply PCB applications. The findings of this study contribute to the ongoing development of efficient, stable, and reliable power electronic systems, ultimately benefiting a wide range of industries that rely on advanced power conversion and management solutions.

II. LITERATURE REVIEW

A thorough review of the relevant literature was conducted to understand the current state of knowledge regarding the impact of ambient temperature on power electronic systems, particularly in the context of BUCK converters, SEPIC converters, and power supply PCB applications. The literature revealed several important findings:

1. Temperature-dependent characteristics of transistors significantly affect the performance and efficiency of power electronic systems [1], [2].
2. Thermal management techniques, such as heatsinks, thermal vias with grounded polygon pour for top and bottom layers, and forced air cooling, play a critical role in ensuring the long-term reliability and stability of power electronic systems [3].
3. Ambient temperature variations can cause changes in the parameters of electronic components, leading to potential issues in system performance and efficiency [4].

These findings indicate that a comprehensive understanding of the impact of temperature on transistors in BUCK converters, SEPIC converters, and power supply PCB applications is essential for optimizing their performance and ensuring long-term reliability.

III. METHODOLOGY

A multi-faceted experimental approach was employed to thoroughly examine the ambient temperature effects on MOSFET and whole circuit, with specific focus on whole through components for board prototype and surface mount components for PCBs. The experimental setup utilized hot air to heat the circuit up to 140˚C and ice bag to cool it down to 0˚C, while an LM35 temperature sensor and an Arduino Uno microcontroller were used to convert the analog voltage to temperature values in Celsius. Output Voltage measurements were taken using a multimeter, and temperature data was collected using the LM35 sensor and Arduino Uno ADC setup. Refer to appendix (A) for the Arduino Uno setup and code.

The BUCK and SEPIC converters were designed, simulated, and implemented using theoretical calculations from relevant textbooks and LTSpice software, respectively. The power supply PCB design was based on the typical example provided in the LTC3850 datasheet, and the PCB layout was created using Altium Designer. These design and simulation tools enabled a comprehensive understanding of the converters' performance under different temperature conditions. The implementation was done in the lab by soldering the components on the board prototype and PCB.

The Buck converter was designed for input voltage 10V, output voltage 5V, 1000 Ω load resistor, and frequency of 100 KHz. Refer to Fig. 1. For the buck converter circuit and appendix (B) for the buck converter design [5].

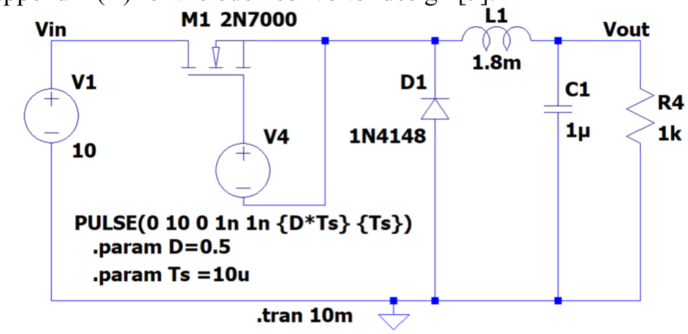

Fig. 1. Buck Converter Circuit (Built in LTSpice).

The SEPIC converter was designed for input voltage of 5V, output voltage range 2.5 to 10V, 500 Ω load resistor, and frequency of 200KHz. Refer to Fig. 2. For SEPIC converter circuit and appendix (C) for the SEPIC Converter design [5].

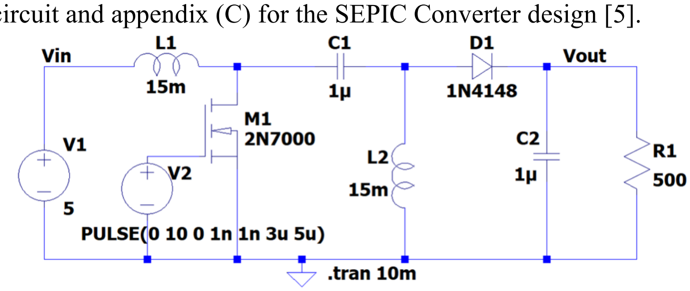

Fig. 2. SEPIC Converter Circuit (Built in LTSpice).

The power supply using IC LTC3850 was designed and implemented for two output voltages of 3.3V and 4V with current up to 2A. The design was done using Altium Designer and soldered in the lab; all components were selected according to the datasheet recommendation and typical examples in datasheet [6]. Refer to Fig.3 for the power supply circuit, which is simulated using LTspice based on the LTC3850 manufacturer and appendix (D) for power supply design including Altium Designer PCB schematic in Fig. 7 and layout in Fig. 8.

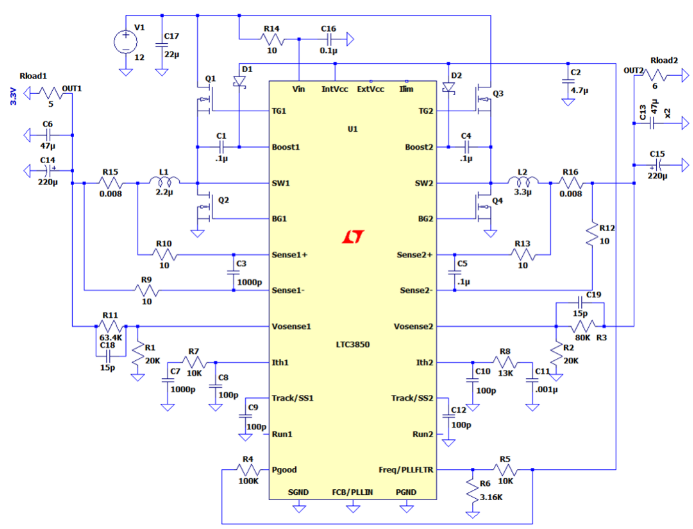

Fig. 3. Power Supply Circuit (Built in LTSpice).

The circuits in Fig. 1 to Fig. 3 were simulated using LTSpice to ensure proper functionality, and the converters are working in continuous current mode (CCM). The prototypes were fabricated and used in the lab for this experiment. Refer to Fig. 4 to Fig. 6 for these converters prototypes and the PCB board in appendix (E).

IV. EXPERIMENTAL RESULTS

The experimental results demonstrated that the output voltage and performance of the BUCK converters, SEPIC converters were affected by the ambient temperature, but power supply PCB has no impact. Specifically, it was observed that:

1. The output voltage of the BUCK increased as the ambient temperature increased. The results are shown in the table I and table II for two types of MOSFETs and plotted as shown in Fig. 9 to Fig. 10. For SEPIC converter, it increases with increasing temperature up to 50˚C and declined when the temperature increases up to 140 ˚C and when cooling it down to 0˚C, the output voltage decreased slightly. The results are shown in the table III and table IV for two types of MOSFETs and refer to the plots in Fig. 11 to Fig. 12.
2. The output voltages of the PCB power supply have no impact when the temperature increased up to 140 ˚C and decreased to 0 ˚C. Refer to the plot in Fig. 13.

A. Buck Converter:

The experimental result involved the characterization of a buck converter under varying temperature conditions to evaluate its performance. The buck converter was subjected to temperature changes using a hot air source and an ice bag. The electrical parameters of the buck converter were set as follows: a period of 10 microseconds (10 µs) corresponding to a frequency of 200 kHz, an output voltage amplitude of 15V with an offset of 2.5V, a duty cycle of 50%, and an input voltage of 10V. The objective was to investigate the impact of temperature on the output voltage of the buck converter. The experiments were conducted using two different MOSFETs, namely the 2N7000 and the IRF1407. The output voltage was measured at various temperatures, including 0°C, room temperature (20°C), and 140°C. The obtained data was plotted and analyzed to assess the temperature sensitivity and performance characteristics of the buck converter. The experimental setup and results are presented in Fig. 9 and Fig. 10 based on the results in table I and table II, which depict the output voltage versus temperature profiles for the 2N7000 and IRF1407 buck converters, respectively. These experiments provided valuable insights into the temperature-dependent behavior of the buck converter, offering valuable information for designing and optimizing its performance in practical applications.

TABLE I
Buck Converter MOSFET 2N7000 Experiment Results.

Output Voltage (V)	Output Current (mA)	Temperature (˚C)	Resistor (kΩ)	Input Voltage (V)	Input Current (mA)
4.71	4.71	0	0.999	10	3.16
4.71	4.71	2.93	0.999	10	3.16
4.72	4.72	20.02	0.999	10	3.17
4.73	4.73	26.86	0.999	10	3.17
4.74	4.74	30.27	0.999	10	3.18
4.79	4.79	39.55	0.999	10	3.2
4.8	4.80	43.46	0.999	10	3.21
4.82	4.82	49.32	0.999	10	3.23
4.84	4.84	57.62	0.999	10	3.24
4.85	4.85	65.43	0.999	10	3.25
4.87	4.87	72.27	0.999	10	3.26
4.89	4.89	80.08	0.999	10	3.26
4.92	4.92	87.89	0.999	10	3.29
4.94	4.94	92.29	0.999	10	3.31
4.95	4.95	100.59	0.999	10	3.31
4.96	4.96	104.49	0.999	10	3.32
4.98	4.98	133.3	0.999	10	3.33
4.99	4.99	136.23	0.999	10	3.34
4.99	4.99	140.63	0.999	10	3.35

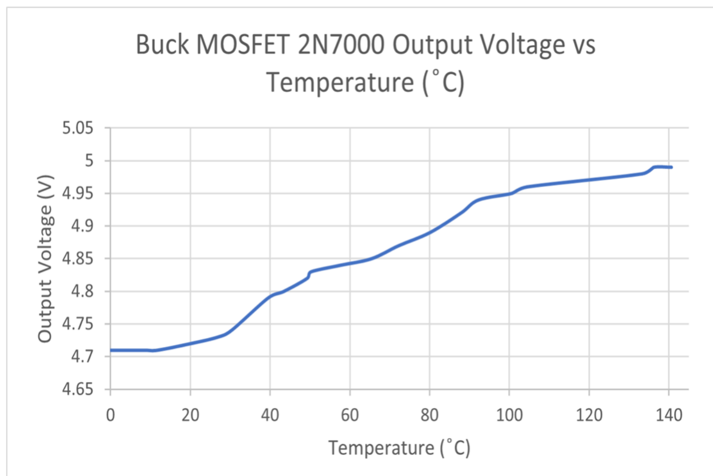

Fig. 9. Buck Converter 2N7000 Plot.

TABLE II
Buck Converter MOSFET IRF1407 Experiment Results.

Voltage (V)	Current (mA)	Resistor (kΩ)	Temperature (C˚)
4.98	5.10	0.977	0
4.99	5.11	0.977	15.9
5	5.12	0.977	19.53
5.01	5.13	0.977	20.02
5.05	5.17	0.977	25.88
5.09	5.21	0.977	33.69
5.1	5.22	0.977	35.16
5.11	5.23	0.977	36.62
5.16	5.28	0.977	46.88
5.19	5.31	0.977	51.76
5.21	5.33	0.977	53.22
5.29	5.41	0.977	70.8
5.3	5.42	0.977	73.73
5.31	5.44	0.977	77.64
5.32	5.45	0.977	79.59
5.33	5.46	0.977	83.98
5.34	5.47	0.977	86.43
5.35	5.48	0.977	90.33
5.4	5.53	0.977	110.35
5.41	5.54	0.977	117.19
5.44	5.57	0.977	131.35
5.45	5.58	0.977	137.21
5.47	5.60	0.977	140

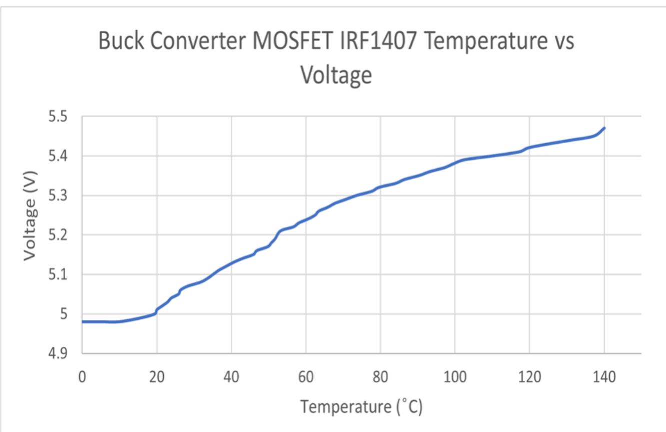

Fig. 10. Buck Converter IRF1407 Plot.

B. SEPIC Converter

In this experiment, a Single-Ended Primary Inductor Converter (SEPIC) was tested under a variety of temperature conditions, using MOSFET 2N7000 and IRF1407, to understand its output voltage response. For a frequency of 100kHz, a period of 10 us, an amplitude of 15V, an offset of 2.5V, a duty cycle of 50%, and an input voltage of 5V, the following results were obtained. For the 2N7000, when the converter was subjected to hot air up to 140°C and cooled to 0°C with an ice bag, the output voltage was observed to increase from 5V (at 0°C) to 5.15V (at up to 121°C). However, at 140°C and room temperature (20°C), the voltage decreased to 5.10V and 5V respectively (refer to figure 3 for the output voltage vs temperature plot). When testing the IRF1407, the output voltage at room temperature (20°C) was 6.31V, which gradually increased to 6.38V at 50.78°C. As the temperature increased beyond 50.78°C, the output voltage began to decline, reaching 6.27V at 140°C. Upon cooling the circuit, the output voltage dropped further to 6.23V at 0°C (refer to table III and table IV and Fig. 11 and Fig. 12 for the corresponding output voltage vs temperature plot). This experiment provides insight into the temperature-dependent behavior of these SEPIC converters using different MOSFETs.

TABLE III
SEPIC Converter MOSFET 2N7000 Experiment Results.

Output Voltage (V)	Output Current (mA)	Resistor (kΩ)	Temperature (˚C)
5	10	0.5	0.98
5	10	0.5	17.09
5	10	0.5	21
5.01	10.02	0.5	25.39
5.03	10.06	0.5	30.27
5.05	10.1	0.5	36.62
5.06	10.12	0.5	40.53
5.07	10.14	0.5	48.34
5.08	10.16	0.5	53.71
5.09	10.18	0.5	58.11
5.1	10.2	0.5	61.04
5.11	10.22	0.5	72.75
5.12	10.24	0.5	76.66
5.12	10.24	0.5	103.03
5.13	10.26	0.5	113.28
5.14	10.28	0.5	117.19
5.15	10.3	0.5	121.09
5.13	10.26	0.5	128.91
5.11	10.22	0.5	136.23
5.1	10.2	0.5	140

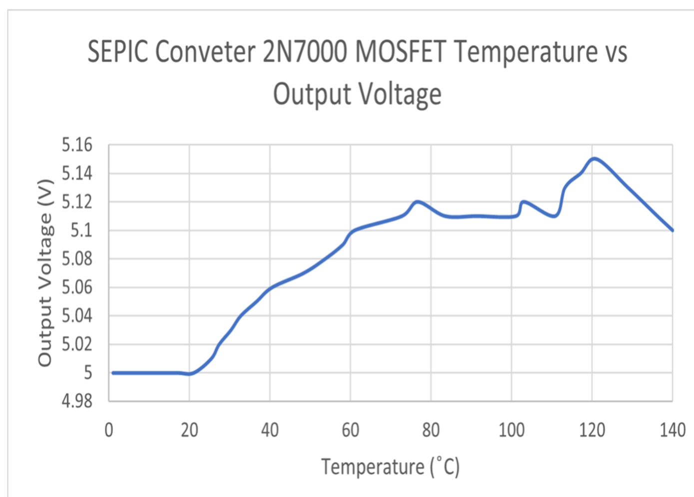

Fig. 11. SEPIC Converter 2N7000 Plot.

TABLE IV
SEPIC Converter MOSFET IRF1407 Experiment Results.

Output Voltage (V)	Output Current (mA)	Resistor (kΩ)	Temperature (˚C)
6.23	12.46	0.5	0
6.24	12.48	0.5	5.37
6.25	12.5	0.5	9.28
6.28	12.56	0.5	15.63
6.31	12.62	0.5	21
6.33	12.66	0.5	25.39
6.35	12.7	0.5	31.25
6.37	12.74	0.5	59.08
6.36	12.72	0.5	79.1
6.35	12.7	0.5	85.45
6.35	12.7	0.5	87.89
6.34	12.68	0.5	96.19
6.33	12.66	0.5	102.05
6.32	12.64	0.5	106.45
6.31	12.62	0.5	110.84
6.3	12.6	0.5	115.23
6.3	12.6	0.5	120.61
6.29	12.58	0.5	131.84
6.29	12.58	0.5	134.28
6.28	12.56	0.5	136.23
6.27	12.54	0.5	141.11

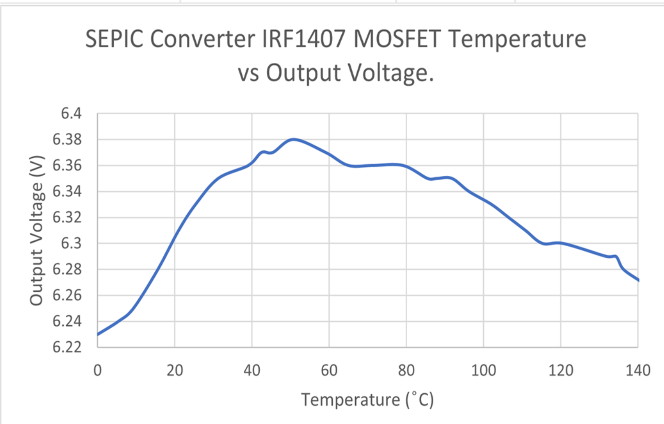

Fig. 12. SEPIC Converter IRF1407 Plot.

C. *PCB Power Supply*

In this investigation, a Printed Circuit Board (PCB) power supply was rigorously assessed, characterized by two distinct output voltages: 3.3V and 4V, across an input voltage range from 4V to 24V. The design of the power supply featured a Dual N-Channel MOSFET Synchronous Drive and a Phase-Lockable Fixed Frequency with an operational bandwidth between 250kHz and 780kHz. An Integrated Circuit (IC) housed in a Shrink Small-Outline Package (SSOP) was also part of the system, and all components employed were of the surface mount variety. Notably, the system demonstrated a remarkable resilience to temperature variations. Experimental data revealed a stable output voltage, unaffected by temperature changes in the range from 0°C to 140°C. This characteristic underscores the robustness and efficiency of the power supply, offering a crucial advantage of not experiencing temperature-dependent voltage variations. Referring to Fig. 13, a graphical representation of the output voltages in response to temperature changes is presented. The linear trajectory of the plot effectively demonstrates the steadfast voltage outputs regardless of temperature alterations, thereby underlining the robust nature of the power supply system studied. Effective thermal management techniques, such as heatsinks, thermal vias, and polygon pours are implemented to dissipate the operating temperature to ensure the long-term reliability and stability of the PCB.

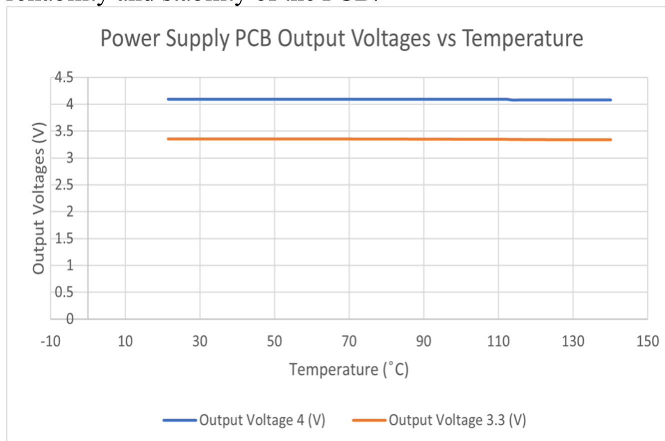

Fig. 13. PCB Power Supply Plot.

V. DISCUSSION

The results of the experimental investigation confirmed the significant impact of ambient temperature on the performance and reliability of transistors in BUCK converters, SEPIC converters applications and has no impact on power supply PCB. The findings revealed that increased ambient temperature led to increasing output voltage and this will decrease converter efficiency and increase conduction losses in the MOSFETs[1, 2].

These observations can be attributed to the temperature-dependent characteristics of transistors, such as the temperature coefficient of resistance (TCR) and the temperature variation of MOSFET on-resistance (RDS(ON)). As the ambient temperature increased, the resistance of the transistors also increased, leading to higher conduction losses and reduced efficiency in the power converters.

The temperature derating factor for components highlighted the importance of maintaining the converters within their specified operating temperature ranges to ensure long-term reliability and stability. Operating the systems at temperatures close to their maximum rated values can result in reduced component lifetimes, emphasizing the need for effective thermal management strategies.

Given the focus on ambient temperature in the study since the junction temperature needs proper tools to measure it, the following equations and formulas related to ambient temperature are important for understanding the impact of temperature on BUCK converters, SEPIC converters, and power supply PCB boards:

1- Temperature Coefficient of Resistance (TCR) equation:

Equation (1) shows the relationship between the change in resistance (ΔR) and the initial resistance (R_0) with respect to the change in ambient temperature (ΔT) , expressed as:

$$\Delta R/R_0 = \alpha * \Delta T \quad (1)$$

Where α is the temperature coefficient of resistance. This helps determine how the resistance of a material changes with respect to the ambient temperature [7, 8].

The load resistor of the Buck converter is 1000 Ω and the SEPIC is 500 Ω ;5% 1/2W, Temperature coefficient + 350 to -450 PPM/°C [9]; the average TCR value, which is the average of the maximum and minimum TCR values. In this case, the average TCR value would be:

Average TCR = (Maximum TCR + Minimum TCR) / 2

Average TCR = (+350 ppm/°C + (-450 ppm/°C)) / 2

Average TCR = -50 ppm/°C

Considering an initial actual resistance R_0 = 977 Ω and 501 Ω respectively at 20°C, a temperature coefficient of resistance α = -50 ppm/°C, and an ambient temperature increase from 20°C to 140°C (ΔT = 120°C), the following calculations can be made using the TCR equation:

For the Buck converter:

$\Delta R/R0 = \alpha * \Delta T$

$\Delta R/977 = -5\times10^{-5} * 120$

$\Delta R = -5.862\ \Omega$

For the SEPIC converter:

$\Delta R/R0 = \alpha * \Delta T$

$\Delta R/501 = -5 \times 10^{-5} * 120$

$\Delta R = -3.006\ \Omega$

Hence, the new resistance value of Buck converter at 140°C: $R_{new} = R0 + \Delta R = 977 + (-5.862) = 971.138\ \Omega$

The new resistance value of SEPIC converter at 140°C: $R_{new} = R0 + \Delta R = 500 + (-3.006) = 496.994\ \Omega$

2- Temperature variation of MOSFET Drain−Source On- Resistance ($R_{DS(ON)}$):

$$R_{DS(ON)}(T_a) = R_{DS(ON)}(25) * (1 + \beta * (T_a - 25°C)) \quad (2)$$

As seen in (2), $R_{DS(ON)}$ (Ta) is the on-resistance at temperature T_a, $R_{DS(ON)}$ (25) is the on-resistance at 25°C, β is the temperature coefficient of on-resistance, and T_a is the ambient temperature. This equation highlights the impact of ambient temperature on the on-resistance of a MOSFET transistor, which is a crucial parameter for the performance and efficiency of power electronic systems, such as BUCK converters, SEPIC converters, and power supply PCB designs.

It describes the temperature variation of MOSFET on-resistance ($R_{DS(ON)}$), which is affected by the ambient temperature [10].

Using the maximum value of 5 ohms for the on-resistance ($R_{DS(ON)}$) to ensure the device's capabilities are not exceeded under extreme temperature conditions [11]. The temperature coefficient of on-resistance β ≈ 0.007 °C^(-1) based on the change of the on- resistance using typical and maximum value provided by the datasheet and the change of ambient temperature from 25°C up to 140°C. It is calculated using the equation below.

$\beta = (\Delta R_{DS(ON)} / R_{DS(ON)})/\Delta T = (5\Omega-1.2\Omega)/(5\Omega)/(140°C-25°C)$

$\beta = 0.0066 \approx 0.007$ 1/°C

$R_{DS(ON)}(Ta) = R_{DS(ON)}(25°C) * (1 + \beta * (Ta - 25°C))$

$R_{DS(ON)}(Ta) = 5 * (1 + 0.007 * (140 - 25))$

$R_{DS(ON)}(Ta) \approx 8.8\ \Omega$

The on resistance of the MOSFETs used in the converters increased with increasing temperature, leading to higher conduction losses, and reducing the efficiency of the power circuit [12, 13].

3- Temperature derating factor for components:

The temperature derating factor is an important consideration for ensuring safe and reliable operation of components in power electronic systems. It considers the impact of ambient temperature variations on the power rating of components. By understanding and applying the derating factor, designers can optimize system performance and reliability.

To calculate the derating factor for the 2N7000 MOSFET, we refer to the power rating versus ambient temperature curve provided in the datasheet. The derating factor is determined using (3):

$$P_D = \frac{T_{C(\max)} - T_C}{T_{C(\max)} - 25} \times P_{D(\max)} \quad (3)$$

Here, P_D represents the power rating, T_c (or T_a) is the case or ambient temperature and $P_{D(max)}$ is the maximum power rating at 25°C. For example, if T_c is 75°C and $T_{c(max)}$ is 150°C, the derating factor is calculated as 0.6W.

Considering a power rating of 1W at 25°C, the new power rating is determined by subtracting the derating factor from 1W. In this case, the new power rating is 0.4W.

Similarly, for a specified ambient temperature of 150°C, the derating factor can be calculated using (4) or (5):

$$D = \frac{P_D}{(T_a - 25\ °C)} \quad (4)$$

$$\text{Or } D = \frac{1}{\theta_{jc}} \quad (5)$$

Using the derived power rating of 0.4W and T_a of 150°C, the derating factor is found to be 3.2mW/°C. Also, the datasheet provides Thermal Resistance or Junction-to-Ambient (θ_{jc}) or (R_{thJA}) to be 312.5°C/W, the derating factor is also found to be 3.2mW/°C. This represents the power derating above 25°C for the 2N7000 MOSFET [11], [14], [15].

For the experiment conducted with a maximum ambient temperature of 140°C, the decrease in power rating (ΔP) can be determined by multiplying the derating factor by the temperature difference (140°C - 25°C). In this case, the decrease in power rating is 0.368W. Therefore, the maximum power dissipation for the Buck converter is calculated as 0.632W.

Considering the temperature derating factor for components is crucial for maintaining safe and reliable operation in the presence of ambient temperature fluctuations. Failure to account for these factors can lead to reduced performance, decreased lifespan, or even component failure. It is important to employ proper thermal management techniques to ensure safe operation within the specified temperature range [15].

Although the circuit may contain other components such as capacitors, diodes, and resistors with different derating factors and temperature ranges, the MOSFET was the main focus of the experiment and experienced the highest temperature impact [16].

By understanding and applying the temperature derating factor for components, designers can ensure that the converters operate within their specified temperature ranges, thus optimizing performance and extending component lifetimes.

By considering these formulas and equations related to ambient temperature, this research can analyze the impact of temperature on transistors in BUCK converters, SEPIC converters, and power supply PCB applications. This information can then be used to provide insights and recommendations for design improvements and thermal management techniques, helping to optimize the efficiency, stability, and reliability of power electronic systems.

Additionally, it is important to consider the temperature impacts on other components commonly found in electronic converters. Inductors, capacitors, and diodes are also subject to temperature dependencies. Inductors experience changes in their inductance value and losses with temperature that can affect the performance and efficiency of the power converter [17]. Capacitors can exhibit variations in capacitance and leakage currents as temperature changes, characterized by the temperature coefficient of capacitance (TCC) [18]. Diodes have temperature-dependent characteristics such as forward voltage drop and reverse leakage current, which impact their conduction and blocking capabilities [19]. Understanding and accounting for these temperature dependencies in inductors, capacitors, and diodes are crucial for accurate design and operation of electronic converters, allowing for optimized system performance, enhanced efficiency, and reliable operation within specified temperature ranges.

VI. CONCLUSION

The impact of ambient temperature on the performance and reliability of transistors in BUCK converters, SEPIC converters, and power supply PCB applications was investigated. The experimental results confirmed that increased ambient temperature led to higher conduction losses and reduced efficiency in the power converters. This behavior can be attributed to the temperature coefficient of resistance (TCR) and the temperature variation of MOSFET on-resistance (RDS(ON)).

To quantify the effects, equations were derived to calculate the change in resistance and on-resistance with temperature. The results showed that the resistance of transistors increased with rising temperature, resulting in decreased converter efficiency. The on resistance of MOSFETs also increased, leading to higher conduction losses.

These findings highlight the importance of maintaining the converters within their specified operating temperature ranges to ensure long-term reliability. Effective thermal management strategies are crucial for optimizing system performance and extending component lifetimes.

Additionally, it is essential to consider the temperature impacts on other components such as inductors, capacitors, and diodes, as they also exhibit temperature-dependent characteristics that can affect converter performance.

By incorporating these insights into design improvements and implementing appropriate thermal management techniques, the efficiency, stability, and reliability of power electronic systems can be enhanced.

In summary, the study confirmed the significant impact of ambient temperature on transistors in power converters and emphasized the need for proper thermal management strategies to ensure reliable operation within specified temperature ranges.

APPENDIX

A- Arduino Uno Setup and Code:

Circuit Connection:

1. **Connect the Vout (output) of the LM35 to A0 (analog input) on your Arduino.**
2. **Connect the GND (ground) of the LM35 to the GND on your Arduino.**
3. **Connect the Vs (power supply) of the LM35 to the 5V output on your Arduino.**

Program to read the analog voltage and convert it to a temperature in Celsius:

```
float temp;
//the setup routine runs once when you press reset:
void setup() {
  // initialize serial communication at 9600 bits per second:
  //analogReference(INTERNAL);
  Serial.begin(9600);
}

//the loop routine runs over and over again forever:
void loop() {
  // read the input on analog pin 0:
  float voltage = analogRead(A0);
  temp=voltage*0.48828125;

  //float temp = sensorValue/10;
  //float temp = 110*avg/1023;
  // print out the value you read:
  Serial.print("Voltage read: ");
  Serial.print(voltage);
  Serial.print(" temp: ");
  Serial.print(temp);

  Serial.println("*C");
  //Serial.println(sensorValue);
```

```
delay(1000);  // delay in between reads for stability every 1000=1 second
}
```

This code reads the voltage from the LM35 sensor, converts it into a temperature reading, and then sends that temperature reading over the serial port. Please note that the Arduino's analogRead() function gives us a value between 0 and 1023, and we convert that to a voltage value by multiplying by 5 (for 5 volts) and dividing by 1024.

B- BUCK converter Design:

Duty Cycle (D) equation:

D = Vout / Vin

D = 5V / 10V = 0.5

Inductor (L) design equation:

L = (Vin - Vout) * D * Tsw / (2 * ΔIL)

Assuming a 20% inductor ripple current (ΔIL) relative to the output current (Io) and an output current of 1A, ΔIL = 0.2 * 1A = 0.2A. The switching period (Tsw) can be calculated as the inverse of the switching frequency (fsw): Tsw = 1 / fsw = 1 / 100kHz = 10µs.

L = (10V - 5V) * 0.5 * 10µs / (2 * 0.2A) = 12.5µH

Capacitor (C) design equation:

C = ΔIL * D * Tsw / (8 * fsw * ΔVout)

Assuming a 1% output voltage ripple (ΔVout) relative to the output voltage, ΔVout = 0.01 * 5V = 0.05V.

C = 0.2A * 0.5 * 10µs / (8 * 100kHz * 0.05V) = 2.5µF

C- SEPIC Converter Design:

The input voltage of 5V, output voltage range of 5V to 6V, and a switching frequency of 200kHz.

Duty Cycle (D) equation:

D = Vout / (Vin + Vout)

D = 5V / (5V + 5V) = 0.5

Inductor (L1 and L2) design equation:

L1 = L2 = Vin * D * Tsw / (2 * ΔIL)

Using the same assumptions as for the BUCK converter, ΔIL = 0.2A, and Tsw = 10µs.

L1 = L2 = 5V * 0.5 * 10µs / (2 * 0.2A) = 6.25µH

Capacitor (C1) design equation:

C1 = ΔIL * D * Tsw / (8 * fsw * ΔVout)

Using the same assumption as for the BUCK converter, ΔVout = 0.05V.

C1 = 0.2A * 0.5 * 10µs / (8 * 100kHz * 0.05V) = 2.5µF

Coupling Capacitor (C2) design equation:

C2 = Vin * D^2 * Tsw / (2 * fsw * ΔVout)

C2 = 5V * 0.5^2 * 10µs / (2 * 100kHz * 0.05V) = 12.5µF

Using the calculated values, you can select the components required for your SEPIC converter design:

L1 and L2: Two inductors, each with a value of 6.25µH
C1: A capacitor with a value of 2.5µF
C2: A coupling capacitor with a value of 12.5µF
These calculations are based on ideal component values.

D- Power Supply design including schematic and layout:

Designing a dual 2-phase synchronous step-down switching controller based on the LTC3850 involves calculation for component values using the datasheet equations, selecting components, and creating a printed circuit board (PCB) layout.

Schematic:

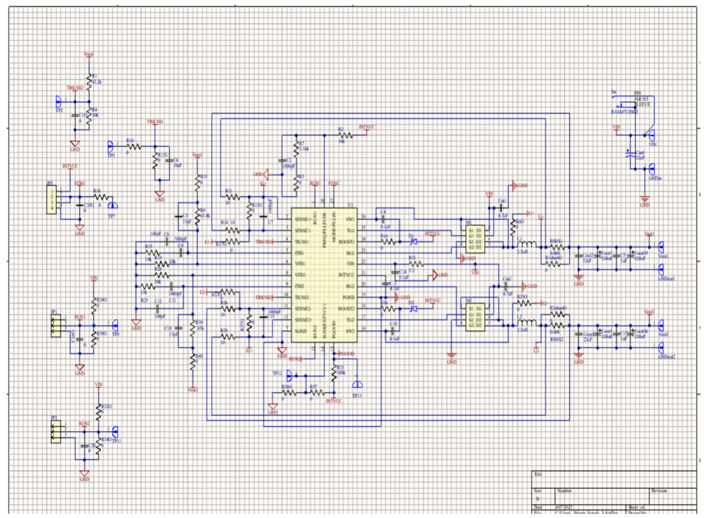

Fig. 7 Power Supply PCB Schematic.

Layout:

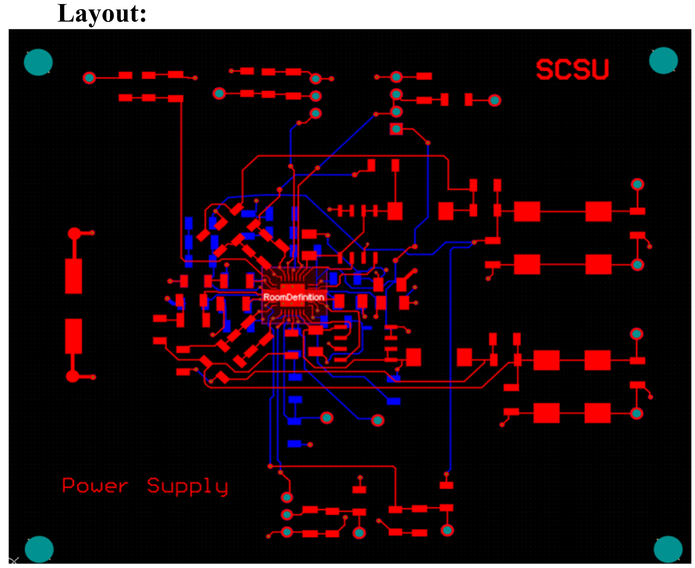

Fig. 8 Signal Trace for Power Supply Layout.

E- Fabricated Boards used for lab experiment:

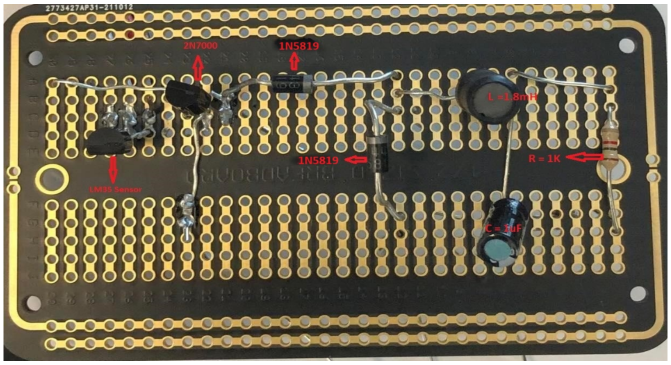

Fig. 4. Buck converter board.

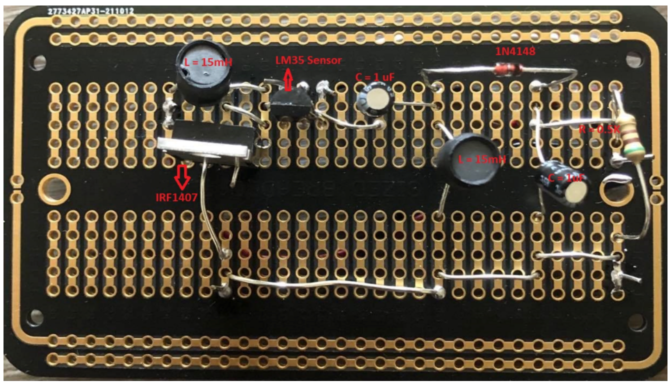

Fig. 5. SEPIC converter board.

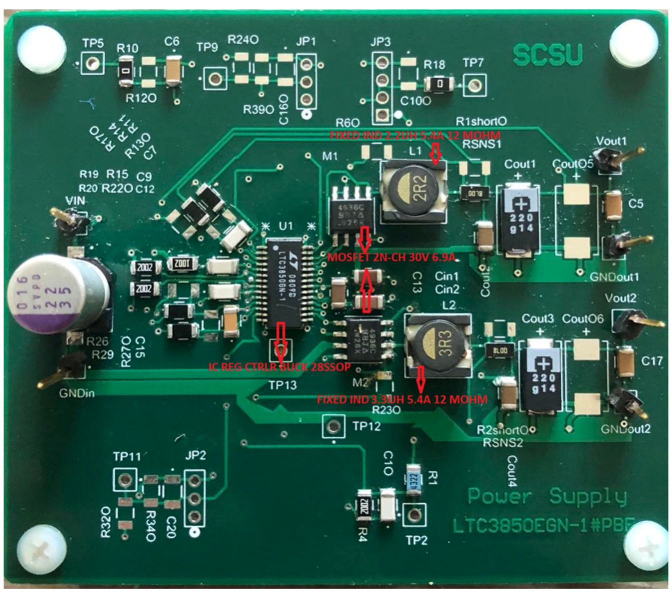

Fig. 6. Power supply PCB board.

Acknowledgment

The author would like to thank the Electrical and Computer Engineering Department at St. Cloud State University for their support in conducting this research.

References

[1] T. Park et al., "Temperature-Dependent Electrical Characteristics of p-Channel Mode Feedback Field-Effect Transistors," in IEEE Access, vol. 10, pp. 101458-101464, 2022, doi: 10.1109/ACCESS.2022.3208116.

[2] A. B. M. H. Talukder, B. Smith, M. Akbulut, F. Dirisaglik, H. Silva and A. Gokirmak, "Temperature-Dependent Characteristics and Electrostatic Threshold Voltage Tuning of Accumulated Body MOSFETs," in IEEE Transactions on Electron Devices, vol. 69, no. 8, pp. 4138-4143, Aug. 2022, doi: 10.1109/TED.2022.3184906.

[3] P. (2021). Circuit Board Thermal Analysis. Altium Resources. Retrieved from https://resources.altium.com/p/circuit-board-thermal-analysis.

[4] D. L. Feucht, Handbook of Analog Circuit Design. Elsevier Inc, Academic Press, 1990, pp. 437-439, ISBN: 978-0-12-254240-4, 0122542401.

[5] D. W. Hart, Power Electronics. New York, NY, USA: McGraw-Hill Education, 2010, pp. 198-211, 231-237, ISBN: 978-0-07-338067-4.

[6] Analog Devices, Inc. (2021). LTC3850 Datasheet and Product Info | Analog Devices. [Online]. Available: https://www.analog.com/en/products/ltc3850.html#product-overview. [Accessed: September 08, 2022].

[7] S. O. Kasap, "Principles of Electronic Materials & Devices," 4th ed., McGraw-Hill Education, 2018, pp. 137-145.

[8] Dennis L. Feucht, “Temperature Effects,” Transistor Amplifiers-Innovatia Laboratories (2014), pp.27-29.

[9] KOA Speer Electronics, "CF Series - Carbon Film Leaded Resistors," [Data sheet]. Available: https://www.koaspeer.com/pdfs/CF.pdf.

[10] R. Perret, Ed., "Power Electronics Semiconductor Devices," 1st ed., Hoboken, NJ: Wiley, 2009, pp. 44-46, ISBN: 978-1848210646.

[11] NTE Electronics Inc., "2N7000 N-Channel Enhancement Mode Field Effect Transistor," [Data sheet]. Available: https://www.nteinc.com/specs/original/2N7000.pdf.

[12] B. J. Baliga, "Fundamentals of Power Semiconductor Devices," 2nd ed. Springer International, 2019, pp. 460-463, Chapter 6 (Power MOSFETs). doi: 10.1007/978-3-319-93988-9.

[13] R. W. Erickson and D. Maksimović, "Fundamentals of Power Electronics," 3rd ed. Cham, Switzerland: Springer, 2020, pp. 1018, Chapter VI (Resonant Converters). doi: 10.1007/978-3-030-43881-4.

[14] Derating of the MOSFET Safe Operating Area - Toshiba-Semicon-storage.com, https://toshiba-semicon-storage.com/info/application_note_en_20180726_AKX00073.pdf?did=59471 (accessed Jun. 1, 2023).

[15] M. K. Kazimierczuk, "Silicon and Silicon-Carbide Power MOSFETs," in Silicon and Silicon-Carbide Power MOSFETs, 2nd ed. John Wiley & Sons Inc, 2015, ch. 18, pp. 880-886, ISBN: 978-1-119-00954-2.

[16] A. Malvino, D. J. Bates, P. E. Hoppe, "Electronic Principles," 9th Edition, McGraw-Hill Education, 2019, Chapter 10: "Power Amplifiers," pp. 403-407. ISBN: 978-1-260-57056-4.

[17] N. Mohan, T. M. Undeland, and W. P. Robbins, "Power Electronics: Converters, Applications, and Design," 3rd ed. John Wiley & Sons, Inc., 2002, ch. 7, pp. 759-760. ISBN: 9780471226932, 0471429082.

[18] A. S. Sedra and K. C. Smith, "Microelectronic Circuits," 7th ed., The Oxford Series in Electrical and Computer Engineering, Oxford University Press, 2014, Chapter 4, pp. 184-207. ISBN: 0199339139, 9780199339136.

[19] B. LEE, I. ABOTHU, P. RAJ, C. YOON, and R. TUMMALA, “Tailoring of temperature coefficient of capacitance (TCC) in nanocomposite capacitors,” Scripta Materialia, vol. 54, no. 7, pp. 1231–1234, 2006. doi:10.1016/j.scriptamat.2005.12.026.